From colour to tissue histology: Physics based interpretation of images of pigmented skin lesions

Ela Claridge[1], Symon Cotton[2], Per Hall[3], Marc Moncrieff[4]

[1] School of Computer Science, The University of Birmingham, Birmingham B15 2TT, U.K.

[2] Astron Clinica, The Mount, Toft, Cambridge CB3 7RL, U.K.

[3] Addenbrooke's Hospital, Cambridge CB2 2QQ, U.K.

[4] West Norwich Hospital, Norwich NR2 3TU, U.K.

Abstract. Through an understanding of the image formation process, diagnostically important facts about the internal structure and composition of the skin lesions can be derived from their colour images. A physics-based model of tissue colouration provides a cross-reference between image colours and the underlying histological parameters. This approach was successfully applied to the analysis of images of pigmented skin lesions. Histological parametric maps showing the concentration of dermal and epidermal melanin, blood and collagen thickness across the imaged skin have been used to aid early detection of melanoma. A clinical study on a set of 348 pigmented lesions showed 80.1% sensitivity and 82.7% specificity.

1 Introduction

Colour is an important sign in the clinical diagnosis of many conditions. In the computer analysis of medical images colour also plays an important role, for example in segmentation and classification. These and similar operations utilise colour as one of the *image features*, but the question "why a particular colour is associated with a particular medical condition" is not frequently asked. How do the colours that we see on the surface arise? Light emitted by a source interacts with the surface and the interior of an object and through these interactions (mainly absorption and scatter) the spectral composition of light is altered. The changes reflect the structure and optical properties of the materials constituting the object and in this sense the light remitted from the object "encodes" its properties. If this encoding is understood, it should be possible to deduce the structure and composition of the object from its colour image.

In this paper we show how the understanding of the image formation process enables us to derive diagnostically important facts about the internal structure and composition of the skin lesions from their colour[1] images. This information is then used for diagnosis of pigmented skin lesions to aid the detection of melanoma.

2 Outline of the method

The key to the interpretation of image colours in terms of the underlying histological parameters is a *model of tissue colouration* which provides a cross-reference between the colour and the histology. This model is constructed by computing the spectral composition of light remitted from the skin given parameters specifying its structure and optical properties. This step needs to be carried out only once. As the mapping between the colours and the parameters is unique for the skin [1], each colour corresponds to one specific set of histological parameters. For each derived parameter a *parametric image* is then created which shows the magnitude of a given parameter at each pixel location. In comparison with traditional methods, this approach to image interpretation requires two additional inputs. One is the set of parameters which characterise a given tissue by specifying its components, their optical properties, their quantities, and their geometry. The other is a method for computing the remitted spectra from the given parameters; in physics terminology "a model of light transport".

Our group has successfully applied this approach to the analysis of images of pigmented skin lesions [2]. Histological parametric maps showing the concentration of dermal and epidermal melanin, blood and collagen thickness across the imaged skin (see Fig. 3) have shown to aid early detection of melanoma [3].

---

[1] In the remainder of the paper "colour" is taken to be a vector of n primaries. For example, a standard colour image is represented by 3 primaries: red, green and blue, i.e. a vector $[r\ g\ b]$.

3 Structure and optical properties of the normal skin

The skin consists of a number of layers with distinct function and distinct optical properties (Fig. 1). White light shone onto the skin penetrates superficial skin layers and whilst some of it is absorbed, much is remitted back and can be registered by a camera.
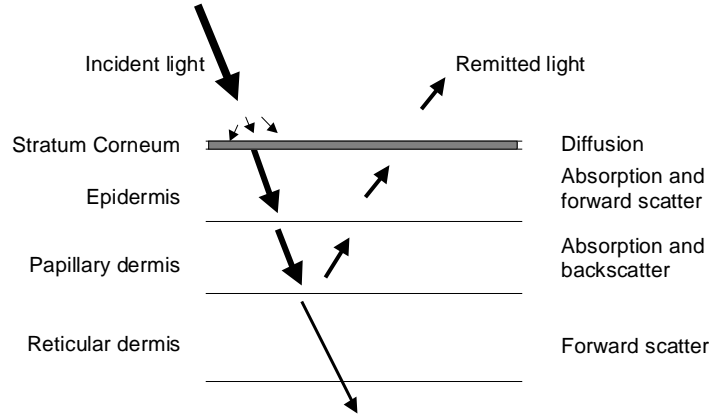

Fig. 1. A schematic representation of the skin layers (names on the left) and their optical properties (on the right). The arrows indicate the path of light through the skin tissues.

The stratum corneum is a protective layer consisting of the keratin-impregnated cells and it varies considerably in thickness. Apart from scattering the light, it is optically neutral.

The epidermis is largely composed of connective tissue. It also contains the melanin producing cells, the melanocytes, and their product, melanin. Melanin is a pigment which strongly absorbs light in the blue part of the visible spectrum and in ultraviolet. In this way it acts as a filter which protects the deeper layers of the skin from harmful effects of UV radiation. Within the epidermal layer there is very little scattering, with the small amount that occurs being forward directed. The result of this is that all light not absorbed by melanin can be considered to pass into the dermis.

The dermis is made of collagen fibres and, in contrast to the epidermis, it contains sensors, receptors, blood vessels and nerve ends. Haemoglobin, present in blood vessels across the whole dermis, acts a selective absorber of light. Dermis consists of two structurally different layers, papillary and reticular, which differ principally by the size of collagen fibres. The small size of the collagen fibres in the papillary dermis (diameter of an order of magnitude less than the incident visible light) makes this layer highly back-scattering; i.e. any incoming light is directed back towards the skin surface. The scatter is greatest at the red end of the spectrum and increases even further in near infrared (nir). As absorption by melanin and blood is negligible in infrared, this part of the spectrum is optimal for assessing thickness of the papillary dermis.

Within the reticular dermis, the large size of collagen fibre bundles causes highly forward-directed scattering. Thus any light which gets to this layer is passed on deeper into the skin and does not contribute to the spectrum remitted from the skin (Fig. 1).

4 Model of colouration for normal skin

From the above analysis, the normal skin can be optically modelled as consisting of three layers:

- epidermis, characterised by the wavelength (λ) dependent set of absorption coefficients for melanin, $\mu_a^m(\lambda)$, and the melanin concentration, c^m;

- papillary dermis, characterised by the absorption coefficients for haemoglobin, $\mu_a^h(\lambda)$, the haemoglobin concentration, c^h, the scatter coefficient for collagen, μ_s^{pd}, and the thickness of the collagen layer, d^{pd};

- reticular dermis, characterised by the scatter coefficient, μ_s^{rd}, and the layer thickness, d^{rd}.

By supplying these parameters and the spectral composition of the incident light $E(\lambda)$ to a model of light transport, the spectral composition of the light remitted from the skin, $R(\lambda)$, can be computed:

$$R(\lambda) = Model\_of\_light\_transport(\ E(\lambda),\ \mu_a^m(\lambda),\ c^m,\ \mu_a^h(\lambda),\ c^h,\ \mu_s^{pd},\ d^{pd},\ \mu_s^{rd},\ d^{rd}\ )$$

In the final step a colour vector [$r\ g\ b\ nir$], is derived from the remitted spectrum $R(\lambda)$ by convolving it with suitable spectral response functions for the red, green, blue and near infrared primaries, $S_R(\lambda)$, $S_G(\lambda)$, $S_B(\lambda)$ and $S_{NIR}(\lambda)$:

$$r = \int_0^\infty R(\lambda)S_R(\lambda)d\lambda,\quad g = \int_0^\infty R(\lambda)S_G(\lambda)d\lambda,\quad b = \int_0^\infty R(\lambda)S_B(\lambda)d\lambda,\quad nir = \int_0^\infty R(\lambda)S_{NIR}(\lambda)d\lambda$$

In this way we can compute the colour of light remitted from the skin's surface.

Parameters in the *Model_of_light_transport( )* above can be subdivided into those which characterise the entire tissue type and those which characterise a specific instance of the tissue. The absorption and scatter coefficients ($\mu_a^m(\lambda)$, c^m, $\mu_a^h(\lambda)$, μ_s^{pd}, μ_s^{rd}) belong to the first group. The thickness of the reticular dermis can be assumed constant because due to its strong forward scattering properties even a thin layer will prevent any remission of light. The levels of melanin and blood concentration c^m and c^h, and thickness of the papillary dermis, d^{pd}, vary for different skin locations. The model captures this variability by computing a set of colour vectors for parameters spanning *the entire range* of histologically valid concentrations and thicknesses. In this way a cross-reference between histology and colour is formed. Expressed as a fragment of a pseudocode, the process of building of the model of colouration can be described as follows:

```
given
     incident light E(λ)
     absorption coefficients of melanin and blood, μₐᵐ(λ), μₐʰ(λ)
     scatter coefficient of the papillary dermis, μₛᵖᵈ
     scatter coefficient and thickness of the reticular dermis, μₛʳᵈ, dʳᵈ
     spectral response functions for the red, green blue and nir primaries,
        Sᵣ(λ), S_G(λ), S_B(λ) and S_NIR(λ)
for all valid concentrations of epidermal melanin, cᵐ
  for all valid concentrations of dermal blood, cʰ
    for all valid thicknesses of papillary dermis, dᵖᵈ
      compute
         R(λ) = Model_of_light_transport( E(λ), μₐᵐ(λ), cᵐ, μₐʰ(λ), cʰ, μₛᵖᵈ, dᵖᵈ, μₛʳᵈ, dʳᵈ )
         colour vector [r g b nir]
```

This forward process computes explicitly tissue colour given a set of histological parameters. As the mapping between the histological parameters and the primaries is unique for the skin [1], the inverse mapping is possible: from the tissue colour to its histological parameters:

$$[r\ g\ b\ nir] \leftrightarrow [\ c^m\quad c^h\quad d^{pd}\ ]$$

The quantities [c^m c^h d^{pd}] are then used to construct parametric maps.

5   Model of light transport

The optical characteristics of the skin tissue are such that a number of different light transport models can be used. We have implemented a two-flux model [5] based on Kubelka-Munk theory [6]. It computes the remitted (R) and transmitted (T) light separately for each layer i: R_i and T_i. For an n layered system, values for $R_{12...n}$ and $T_{12...n}$ are computed recursively [7]:

$$R_{12...n} = R_{12...n-1} + \frac{T^2_{12...n-1}R_n}{1 - R_{12...n-1}R_n}$$

and

$$T_{12...n} = \frac{T_{12...n-1}T_n}{1 - R_{12...n-1}R_n}$$

The model for the normal skin has three layers, corresponding to epidermis, upper papillary dermis (with prevalence of blood) and lower papillary dermis. All the absorption and scatter coefficients are based on the published data (e.g. [4]). The range of wavelengths, from $\lambda = 400$ to 1200 nm, covers the whole visible spectrum and a small range of near infrared radiation. The wavelengths used for computations are taken at equal intervals of 30nm, giving 30 discrete points for each spectrum. The incident light is "white", i.e. it has equal contributions from each discrete wavelength. The $[r \quad g \quad b \quad nir]$ vectors are derived from the computed spectra using a set of response functions equivalent to physical filters used by a camera. Figure 2 represents schematically the relationship between the two reference systems: colour, $[r \quad g \quad b]$; and histological parameters: melanin concentration, blood concentration and thickness of the papillary dermis, $[c^m \quad c^h \quad d^{pd}]$.

Recently the model has been verified by comparing its output to the output generated by a stochastic Monte-Carlo method using a public domain implementation by Prahl *et al* [8].
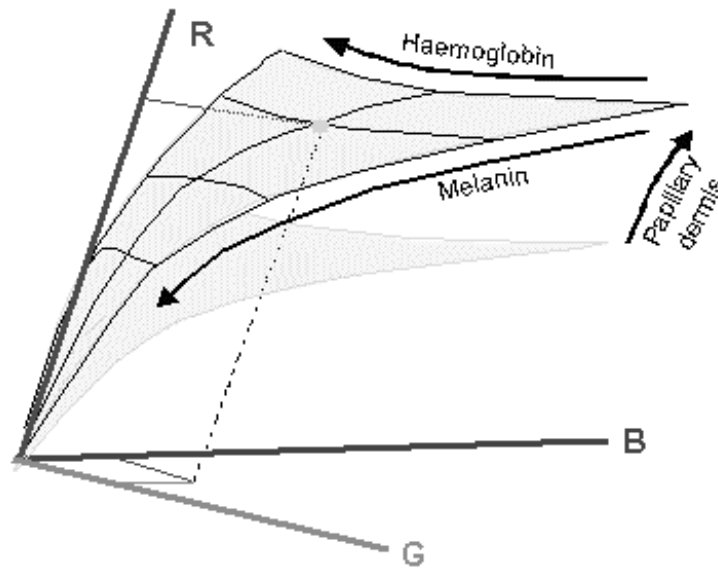

Fig. 2. Schematic relationship between two reference systems: colour system, with axes R, G and B; and histological parameter system, with axes Haemoglobin, Melanin and Papillary Dermis.

6 Abnormal skin

The model above has been constructed for skin which has a normal structure. Skin colouration associated with abnormal conditions does not necessarily have to conform to this model and this has been found to be true for some classes of pigmented skin lesions. We shall review briefly the characteristics of common lesions and discuss the implications of their structure on the model of colouration.

Pigmented skin lesions appear as patches of darker colour on the skin. In most cases the cause is excessive melanin concentration in the skin. In benign lesions (e.g. common naevi) melanin deposits are normally found in epidermis. Excessive pigmentation can also occur as the result of the papillary dermis becoming thin (light instead of being back-scattered is absorbed by structures beyond the reticular dermis). Sometimes small deposits of blood or large concentrations of small blood vessels can take the appearance similar to a pigmented skin lesion. All these types of lesions conform to the "normal" skin model, frequently at the high end of pigment concentration ranges or low end of the thickness range.

Malignant melanoma occurs when melanocytes reproduce at the high, abnormal rate. Whilst they (and their associated melanin) remain in the epidermis, melanoma is termed "in situ". At this stage it is not life-threatening and its optical properties make it conform to the "normal" model of colouration. When malignant melanocytes have penetrated into the dermis, they leave melanin deposits there, changing the nature of skin colouration. The likelihood of metastases increases with the depth of penetration and patient prognosis becomes increasingly worse. Sometimes dermal melanin is found also in benign lesions (e.g. junctional naevus and blue naevus).

The colour of the skin with melanin deposits in the dermis no longer fits the model of normal colouration. This non-conformance to the model marks it as being "abnormal" and provides a highly sensitive diagnostic sign. Such abnormal colours are marked on a fourth parametric map which shows the presence of melanin in the dermis.

The presence of melanin in the dermis is the most significant sign of melanoma. However, it cannot be used as a sole diagnostic criterion because *in situ* melanomas do not have dermal melanin; moreover, some naevi have dermal deposits (although their spatial patterns tend to be more regular than in melanoma). Other signs, some of which can be indicative of melanoma *in situ*, are thickening of the collagen fibres in the papillary dermis (fibrosis); increased blood supply at the lesion periphery (erythematous reaction); and lack of blood within the lesion, in the areas destroyed by cancer. All these signs can be captured in the parametric maps. Figure 3 shows an image of a lesion (a melanoma) and the four parametric maps.
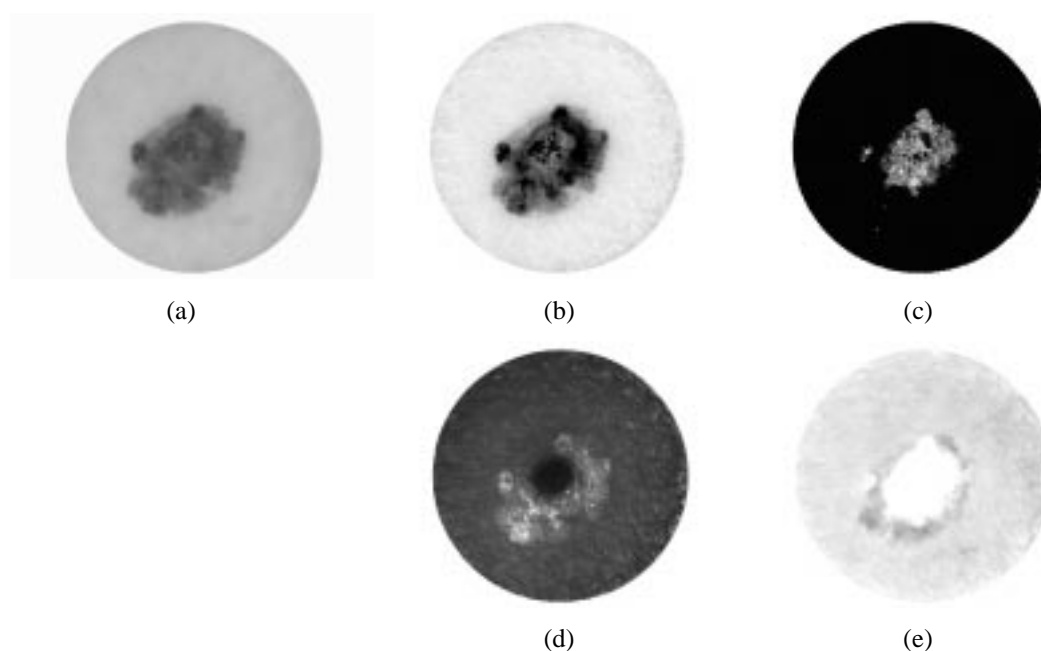

(a)   (b)   (c)

(d)   (e)

Fig. 3. (a) A colour image of a melanoma; Parametric maps showing (b) total melanin; (c) dermal melanin (note that dermal melanin is present); (d) thickness of the papillary dermis (note the increased amount on the periphery and also a "collage hole" in the centre of the lesion where collagen was displaced by melanin); (e) blood (note the absence of blood in the centre of the lesion - white area - and increased amount of blood on a periphery - an erythematous reaction).

6   Clinical evaluation

This method was evaluated in a clinical study at the Addenbrooke's Hospital, Cambridge, and at the Norwich Hospital. The objective of the study was to see whether the histological features which can be directly observed in parametric maps improve diagnosis of melanoma in comparison to standard clinical examination.

A set of 348 lesion images was collected inspecialized dermatology clinics in Cambridge and Norwich using a SIAscope [9], see figure 4. Lesions were scored according to a revised seven-point checklist [10] – a standard method in clinical assessment of lesions. Each imaged lesion was then excised and sent for histolopathological analysis. Histology reports (melanoma vs. non-melanoma) were taken to be the ground truth. The set included 52 melanomas of various sub-types and at various stages of development. Most of the non-melanomas were benign naevi. Factual and clinical information was also recorded, including gender, location on the body, diameter, symmetry and others.

The parametric maps of the lesions, together with their clinical information and colour images, were examined visually by an experienced clinician. This preliminary analysis [3] identified the features listed in Table 1 as being most strongly associated with melanoma. The table lists also sensitivity and specificity of the individual features.

Fig. 4. SIAscope – a certified commercial device developed using the model of skin colouration described in this paper.

Table 1. Diagnostic features associated with the parametric maps, and sensitivity and specificity of the individual features in melanoma classification.

Diagnostic feature	Parametric map	Sensitivity (%)	Specificity (%)
Presence of dermal melanin	Dermal melanin	96.2	56.8
Areas within the lesion with no blood present ("blood displacement")	Dermal blood	75.0	70.3
Increase in blood level on the lesion periphery ("erythematous blush")	Dermal blood	75.0	65.5
Areas within the lesion with no collagen present ("collagen holes")	Collagen thickness	78.8	74.0
Asymmetry	Total melanin	76.9	62.2

The subsequent logistic regression analysis identified the combinations of the features which result in the best overall classification of melanoma [3]. Figure 5 shows ROC curves for two best combinations. A curve for a clinical diagnosis based on a revised seven-point checklist is included for comparison.

7   Discussion and conclusions

The classification results of 80.1% sensitivity and 82.7% specificity compare very well with other diagnostic methods (clinical diagnosis [10] and dermatoscopy [11]). This can be attributed to the fact that the parametric maps provide a clinician with information which can be easily understood and interpreted because it is directly related to histology.
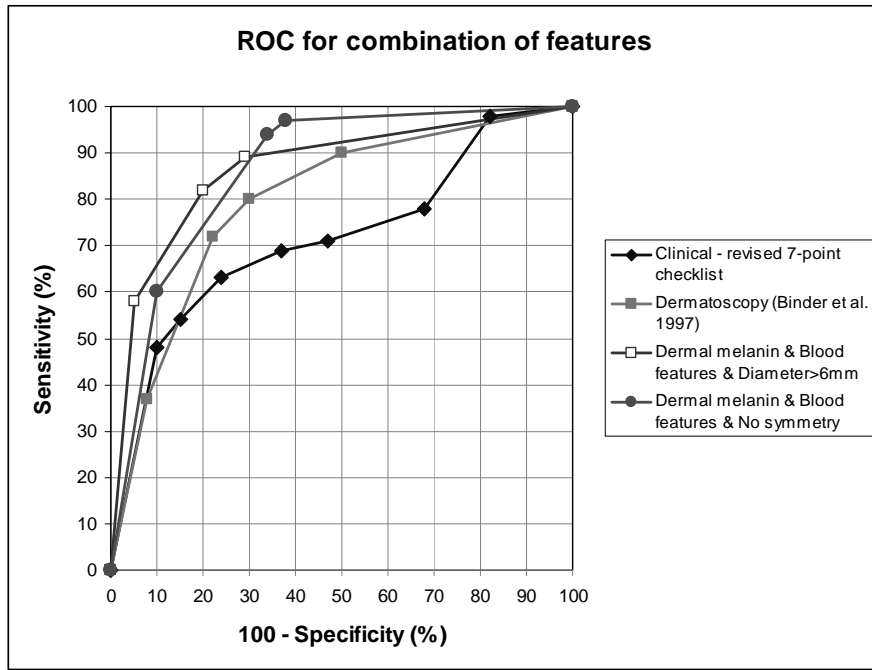
ROC for combination of features

Fig. 5. Receiver-operator characteristic (ROC) curves for combinations of features, compared with clinical assessment and dermatoscopy.

Traditional computer based techniques for the analysis of pigmented skin lesions all aim to correlate the lesion's appearance with its diagnosis. Visual features are usually based on the published "checklists" [12] [13], and include colour, pigmentation, pigment variation, border irregularity, asymmetry, size etc. The methods differ in the way that the measurements of these features are derived from digital images and the way that they are correlated with diagnosis ([14]-[18]). However, they lack explanatory power and in most instances act as "black boxes" which take in the images and output either numerical parameters or a putative diagnosis. Systems of this nature are not well accepted by practicing clinicians.

Our approach is fundamentally different in two ways. First, it does not concentrate on *image* patterns and *image* features, but through a physics-based interpretation of image colours it makes explicit the underlying *histology*. Second, by generating images showing relative magnitudes of the histological entities, the lesion appearance can be correlated with its structure, thus providing an *explanation* as to why various skin diseases manifest themselves through particular visual signs. The model of normal skin colouration is representative of *all* the normal skins, irrespective of racial origin, age or gender [5]. The structure remains the same, and the only differences are in the magnitudes of the parameters c^m, c^h, and d^{pd}.

Colour changes of many body tissues are used for diagnosing diseases. Most tissues have regular laminar structure, collagenous framework and contain a small number of pigments. The colour interpretation method presented in this paper can be clearly extended to other tissues and in some cases it may be an attractive alternative to biopsy.

References

1. Cotton SD (1998) *A non-invasive imaging system for assisting in diagnosis of malignant melanoma*. PhD Thesis, School of Computer Science, The University of Birmingham.

2. Cotton SD, Claridge E, Hall PN (1997) Noninvasive skin imaging, *Information Processing in Medical Imaging* (Springer-Verlag, LNCS 1230), 501-507.

3. Moncrieff M, Cotton S, Claridge E and Hall PN (2002) Spectrophotometric Intracutaneous Analysis: a new technique for imaging pigmented skin lesions. *British Journal of Dermatology* 146(3), 448-457.

4. Anderson R, Parrish BS, Parrish J (1981) The optics of human skin. The Journal of Investigative Dermatology 77(1), 13-19.

5. Cotton SD, Claridge E (1996) Developing a predictive model of human skin colouring, Vanmetter RL, Beutel J Eds., *Proceedings of the SPIE Medical Imaging 1996* vol. 2708, 814-825.

6. Egan WG, Hilgeman TW (1979) *Optical Properties of Inhomogeneous Materials*: Academic Press.

7. Spiegel MR (1962) *Theory and Practice of Advanced Calculus*: McGraw-Hill.

8. Prahl S A, Keijzer M, Jacques S L and Welch A J 1989 A Monte Carlo Model of Light Propagation in Tissue *SPIE Institue Series IS* **5** 102-11.

9. http://www.siascope.com

10. Morton CA, MacKie RM (1998) Clinical accuracy of the diagnosis of cutaneous malignant melanoma. *British Journal of Dermatology* 138, 283-287.

11. Binder M, Puespoeck-Schwarz M, Steiner A et al (1997) Epiluminescence microscopy of small pigmented skin lesions: short-term formal training improves the diagnostic performance of dermatologists. *Journal of the American Academy of Dermatology* 36, 197-202.

12. MacKie R (1985) *An illustrated guide to the recognition of early malignant melanoma*. University Department of Dermatology, Glasgow.

13. ABCDE system of the American Cancer Society - "Asymmetry, Border, Colour, Diameter and Elevation".

14. Ercal F, Chawla A, Stoecker W, *et al.* (1994) Neural network diagnosis of malignant melanoma from color images. *IEEE Transactions on Biomedical Engineering* **41**, 837-845.

15. Bono A, Tomatis S, *et al.* (1996) Invisible colours of melanoma. A telespectrophotometric diagnostic approach on pigmented skin lesions. *European Journal of Cancer* **32A**, 727-729.

16. Menzies S, Crook B, McCarthy W, *et al.* (1997) Automated instrumentation and diagnosis of invasive melanoma. *Melanoma Research* **7**, 13.

17. Ganster H, Pinz A, Kittler H, *et al*. (1997) Computer aided recognition of pigmented skin lesions. *Melanoma Research* **7**, 19.

18. Elbaum, M, Kopf AW, Rabinovitz HS *et al* (2001) Automatic differentiation of melanoma from melanocytic naevi with multispectral digital dermoscopy: A feasibility study. *Journal of the American Academy of Dermatology* 44(2) 207-218.